IEEE Access
Multidisciplinary | Rapid Review | Open Access Journal

Received May 5, 2020, accepted May 14, 2020, date of publication May 19, 2020, date of current version June 2, 2020.

Digital Object Identifier 10.1109/ACCESS.2020.2995650

Impact of Seasonal Conditions on Vector-Borne Epidemiological Dynamics

MD ARQUAM[1], ANURAG SINGH[1], (Senior Member, IEEE), AND HOCINE CHERIFI[2]
[1]Department of Computer Science and Engineering, National Institute of Technology Delhi, New Delhi 110040, India
[2]Department of Computer Science, University of Burgundy, 21078 Dijon, France

Corresponding author: Anurag Singh (anuragsg@nitdelhi.ac.in)

ABSTRACT Vector-borne diseases such as malaria, dengue fever, West Nile virus, and so forth are some of the most prominent threats to human health. They are transmitted to the human population by infected insects or by direct transmission between humans. The epidemic process relies on suitable environmental and climatic conditions. Indeed, climatic factors affect the development of pathogens in vectors as well as the population dynamics of the vectors impacting significantly the incidence of disease in the human population. While the influence of the climatic conditions on Vector-borne diseases is well-documented, there is a strong need to design more realistic epidemiological models incorporating environmental features that show a close relationship with the epidemic process observed in the human population. Indeed, classical models concentrate either on the climatic influence on the vector population dynamics or on the connectivity patterns of the host population, loosing the full picture of the epidemic process dynamics. Inspired by real data of infectious diseases, a Seasonal Susceptible-Infected-Recovered (Seasonal SIR) epidemiological model is developed and analyzed. The proposed model incorporates the influence of the temperature variations together with the heterogeneous structure of the human interaction network on the spreading process of vector-borne diseases. Simulations are performed in order to get a better understanding of the climate variations and of the heterogeneous nature of the contact network on the transmission dynamics. Results show that failing to incorporate these features on the model can lead to a poor estimation of the maximum fraction of infected individuals in the host population. Furthermore there is a serious influence on the time needed to reach this maximum. The Seasonal SIR model proves to finely model the dynamics of outbreaks observed in real-world situations. It provides a basis for more effective predictions of disease outbreaks that can be used in order to implement appropriate control measures to contain epidemics.

INDEX TERMS Vector-borne diseases, epidemics, heterogeneous contact network, climate variations, dynamics on networks, SIR model, epidemiological models.

I. INTRODUCTION

Some contagious diseases are transmitted through both direct and indirect interactions between two populations. Direct transmission occurs when a healthy (susceptible) person is infected by physical or close contact with an infected person of the host population. An indirect transmission refers to the case where a healthy person is infected through a vector population. Vectors are living creatures that transmit infection of pathogens between humans or from animals to humans. Common vector-borne diseases include Zika, Malaria, Dengue, Chikungunya, West Nile Fever. Their transmission process relies on complex interactions between the host population, the vector population (insect species mosquitoes, ticks, flies, sandflies, fleas and bugs), and various pathogens.

The main route of transmission of Vector-borne diseases is trough vectors, however, in some cases direct transmission between two people can occur. For example, there has been substantial evidence of sexual transmission of zika Virus [1]–[4]. CCHF(Crimean-Congo haemorrhagic fever) is primarily transmitted to people from vector. However, human-to-human transmission can occur resulting from close contact with the blood, secretions, organs or other bodily fluids of infected persons [5]. Researchers are suspecting the role of vector in ebola transmission as well as direct transmission between two people [6].

The associate editor coordinating the review of this manuscript and approving it for publication was Zhan Bu.

Vector-borne diseases significantly affect human health worldwide. According to the World Health Organization, more than 120 million cases of vector-borne diseases are reported annually, causing 1 million death. These diseases develop rapidly throughout the world. Indeed, nowadays more than 120 countries, and approximately 60% of the world population [7] are at risk of these types of diseases. Understanding the interdependence between host, vector, and pathogen in order to design effective control strategies is one of the major societal challenges. Although the world has seen the reduction of many infectious diseases in recent decades with the advances in medical care and treatment, the global incidence of vector-borne diseases has increased. Indeed, periodical epidemics have been observed in the last three decades.

Global Warming is a key element of the development of vector-borne diseases. As temperature rises, the threat of vector-borne diseases such as Dengue, Zika, West Nile Fever, and Chikungunya is expanding to temperate areas. Besides global warming,local environmental conditions such as temperature, precipitation, and humidity are also important features affecting the development of vector-borne diseases. The complex interactions between the three players (host population, vector population, pathogens) of vector-borne diseases are very sensitive to environmental conditions. In particular, the development, reproduction and behavior of vectors are highly influenced by climatic conditions [8]. The reproduction rate of vectors increase in warm areas [9]. Other factors such as natural surroundings demolition, land use, pesticide campaign, impact the vector behavior (especially the biting rate) throughout the year. Temperature also can affect pathogen development within vectors. Concerning the host population, the interactions within the individuals, their mobility and connection patterns are essential components in the propagation process of infectious diseases. Indeed, the expansion of urban areas together with the increasing human mobility over the last decades accelerates the diffusion of epidemic waves throughout the world.

A lot of mathematical frameworks inspired by the contagion patterns of observed epidemic scenarios have been proposed in order to predict future epidemics and to assess the impact of immunization and control strategies. In the vector-borne disease framework, they can be classified according to the emphasis they give either on the characteristics of the vector population or of the host population.

Early work of Ross [10] is one of the most influential at the basis of the quantitative foundations of epidemiology. He proposed a transmission model of human-vector crossed contagions for malaria. The model enriched by Macdonald [11] has influenced both the mathematical development of new models and the design of control strategies of vector-borne diseases [12], [13]. Since then, their work has been enriched by the constant refinement of the so-called RossMacdonald model. As temperature is one of the main environmental factor with a direct impact on vector-borne diseases, a great deal of work are conducted to study its influence on the epidemiology of vector-borne diseases. However, these works focus mainly on the impact of the temperature on the vector population dynamics. Indeed, the most common strategy to eradicate vector-borne diseases is to control the vector population. While these works generally acknowledge that the pattern of interactions in the host population is an important factor for vector-borne diseases transmission, they neglect this aspect. In line with classical epidemic models, they assume that all the individuals forming the host populations have homogeneous characteristics.

In recent years, a number of mathematical models that account for the fact that diseases spread over an heterogeneous contact network of the host population have been proposed and analyzed. Incorporating human connectivity and mobility patterns into the disease transmission process, these refined models allow designing new strategies to contain epidemics spreading. Unfortunately, except for a few cases, these models deal principally with a direct transmission scenario neglecting the vector-borne disease framework. Therefore, intensive researches integrating recent advances on the impact of environmental conditions on the vector population together with the influence of the heterogeneity observed in the host population in vector-borne diseases dynamics are required. Indeed, understanding the complex interdependency between human activity and environmental conditions of the vector population is essential to explain the development of large-scale epidemics of vector-borne diseases. New models considering the dual-route of spreading between host and vector population, the environmental conditions as well as the contact structure of the host population are needed. There is an urgent need to control the threat of vector-borne diseases such as Zika and Chikungunya on the world population lives. Therefore, designing an adequate model for the spreading pattern of disease through vector-host interaction as well as host-to-host interaction and climatic environmental conditions is a must to achieve this goal.

In view of these considerations, a Seasonal SIR model that incorporates relevant features of the vector and the host population in the transmission process is proposed and systematically analyzed in order to understand its complex dynamics. This model considers both the impact of temperature and the network structure of the host population on the epidemic dynamics. In a preliminary work [14] an homogeneous contact network (Small-World Network) has been used to model the interactions in the host population. In the current work, we take the model one step further by relaxing the homogeneous contact network assumption. We consider the heterogeneous contact behavior observed in most real-world networks. Indeed, in an homogeneous contact network, each host has a similar number of connectivity, while in a realistic scenario the connectivity patterns of the hosts are generally quite different. Most empirical studies reported in the literature on the topology of real-world networks show that there is a small number of nodes that are highly connected, while the vast majority of nodes have few

connections. This heterogeneous nature of the distribution of the number of contact is well approximated by a power-law distribution [15]–[19].

Our goal is not to focus on any vector-borne disease in particular. Investigating a generic model that account for common properties shared by various vector-borne diseases allows getting a clear idea of the influence of both temperature and heterogeneity of the host population.

The main contributions of this study are as follows.

First of all, we propose a new model in order to improve the understanding of vector-borne diseases dynamics in realistic situations. Under the mean-field formalism, we provide analytical results to assess the impact of both the temperature and the contact network topology on the Seasonal SIR model dynamics.

Second, we conduct an extensive investigation of the Seasonal SIR model to analyze the influence of its various parameters on the epidemic spreading process. The simulations are performed under the assumptions that the contact network can be approximated by the Barabasi-Albert Model (B-A) [20], [21], and that the biting rate of the vectors is a Gaussian function of the temperature. Additionally, comparisons with a temperature-independent model and an homogeneous contact network model are conducted. We also derive an analytical expression of the basic reproduction number that captures the critical conditions leading to epidemics.

Finally, through an improved understanding of transmission dynamics, we show that the proposed model has the potential to predict more accurately seasonal patterns observed in vector-borne diseases and to provide a basis for more efficient treatment and control measures.

The remaining part of this paper is structured as follows. Section II describes the related works. Studies dealing with either the climatic impact on the vector population or the interaction patterns of the host population are presented. Section III present the proposed model and its mathematical formulation using the mean-field formalism. Numerical simulations of the proposed model and the analysis of the results are discussed in section IV. At last, the conclusions and future research directions are described in section V.

II. RELATED WORKS

In this section, first, various remarkable results related to the impact of climatic factors on the vector population dynamics are reported. Works departing from the classical assumption of well-mixed population for the host population based on the metapopulation concept are also presented. Then, we turn to studies that specifically model the heterogeneous nature of the individuals in the host population. These studies pave the way for more realistic models that explore simultaneously the influence of the climatic conditions on the vector population and the heterogeneous nature of the interactions in the host population in vector-borne diseases.

A. INFLUENCE OF ENVIRONMENTAL FACTORS ON VECTOR-BORNE DISEASES

To predict the dynamics of vector-borne diseases in the host population, one must understand the ability of the vectors to transmit the disease under various environmental conditions. Many researchers have studied the relationship between the vector population dynamics and the conditions of their habitual environments. Indeed, environmental conditions may affect the vector population, and in turn the period of existence, the range of spreading and the intensity of disease. Temperature is one of the main environmental variables influencing vector-borne disease dynamics. For a complete review of the temperature dependence of transmission across vectors, pathogens, and environment, the reader can refer to [22]. Field-based experimental data across different vector species that transmit different pathogens show that various features such as biting rate, relative fecundity, mosquito development rate exhibit similar sensitivity to temperature variations. A key principle of thermal biology is that the effects of temperature on mosquito-borne disease transmission are unimodal with lower and upper limits. Starting at zero for a lower temperature limit, their value increase with the temperature until a maximum, then it starts to decrease until an upper temperature limit is reached [23]. Such behavior can be well approximated by a Gaussian distribution. Harvell *et al.* stated that some infectious diseases like Malaria, Red Fever and Dengue are expanding their territories due to the global warming, pushing vectors to move from lower latitude to higher latitude [24]. Temperature variation limits the distribution as well as the density of vectors. For example, dengue fever vectors is at the larval state at $34°C$, and adult vector dies when the temperature is above $40°C$ [25]. Literature also suggests that temperature has also an impact on the life cycle of pathogens, especially reproduction and extrinsic incubation period affecting disease dynamics [24], [26]–[28]. Environmental changes may affect positively the dynamics of water-borne infectious diseases during rainfall [29]. However, it does not always provide favourable condition for the survival of vector. Indeed, heavy rain can have a catastrophic impact on the vector population by sweeping the breeding site of vectors [30]. In contrast, dryness in humid regions provides the best option and propitious condition for vectors to breed and grow [31]. Yang *et al.* proposed a model to study the impact of seasonal variation on the incidence of Dengue [32]. In their research, the authors performed temperature-controlled experiments explaining the impact of varying temperature on the mosquito life-cycle. Andrea Egizi *et al.* gave the experimental proof that the vector population is capable of rapid evolution because of their habitat changes. They suggest to incorporate this characteristic into models of vector-borne disease [33]. Paul E. Parham *et al.* explained the theoretical approach on the impact of environmental changes on vector-borne sicknesses of people [34]. Lindsay P. Campbell *et al.* investigated the impact of environmental changes on worldwide dispersion of vectors involved in Dengue and Chikungunya. They contemplated and inspected

the worldwide potential dispersion of Aedes aegypti and Aedes albopictus in connection to climatic conditions worldwide to create environmental speciality models [35].

In parallel with this very substantial body of work, there have been some attempts to incorporate the host population mobility features into the framework of vector-borne diseases using the meta-population concept. The goal of this approach is to represent the disease transmission process involving a set of cities or patches that can be visited by hosts. The populations belonging to the various patches are considered well-mixed. Infected host can transmit the disease to susceptible host in other patches either by short visits from their home or by migrating to another patch.

Moon et al proposed a spatio-temporal framework for the spreading of West Nile virus using three distance dispersal kernal model considering short-range dispersal, long-range dispersal and flyway direction of mosquitoes. Authors suggested that flyway direction kernel is the best kernel to fit WNV human case data [36]. Sekamatte et al studied the spreading of Rift Valley fever using individual based network model. Rift Valley fever is spread through mosquito to livestock and wildlife but also affect humans. Author suggested that spatial spread of Rift Valley fever can be controlled by restricting the cattle movement during the periods of high mosquito abundance [37] Ferdousi et al proposed an indivual based interconnected network model to explain the both route of transmission of zika virus as through vector-human interaction as well as human-human interaction. They claimed that survival probability of zika virus is high in the human population. Authors suggested that zika outbreaks are impacted by time of introduction of pathogen, proportion of available indivdual and their transmissibility [4].

Wang *et al.* study the spreading process between two patches where host can migrate from one patch to another [38]. Their SIS model incorporates differences between the migration rates of susceptible and infected individuals. They give the various situations leading to persistence or extinction of the disease according to the migration conditions. Arino *et al.* proposed a multiple-route epidemic model to investigate the dynamics of vector-borne disease in human population considering the travel pattern of an infected individual between different geographical region [39], [40]. Their model consider N patches and short visits between patches so that the patches population is constant. Their results are quite comparable with the work of Wang and Mulone [38]. Auger *et al.* extended the Ross-Macdonald model to a meta-population setting [41]. They assume that the hosts can migrate but vectors do not migrate. The migration rate of the hosts is constant and independent of the host status (Susceptible or Infected). They also assume that the epidemiological parameters are identical for all the patches. Results of an extensive investigation of the influence of the various parameters on the spatial and temporal epidemic dynamics are reported. More recently Soriano-Paños *et al.* [42] proposed a multi-patches Ross-Macdonald model in the same vein. Considering short visits between the patches, it incorporates a human mobility model and a variable vector population size. Under these assumptions they derive the epidemic threshold and an indicator allowing to measure the risk for the patches to be affected by the disease. In order to study the dynamics of Dengue, Phaijoo and Gurung [43] proposed a multi-patch SIR-SI model where individuals can migrate to different patches. The disease prevalence is assumed to be variable for the different patches and the mobility rate between patches is also variable in their model. They show that reducing exchanges from highly infected patches to low infected patches can help controlling the disease.

B. INFLUENCE OF THE HETEROGENEITY OF THE HOST POPULATION

Classical epidemic models describe the dynamics of infections at the population level. They consider that the entire population is divided into a number of sub-populations that share the same state. For example, in the basic SIR model, the population is divided into three compartments (Susceptible, Infected, Recovered) and the dynamics consist of following the evolution of the size of each sub-population. The underlying assumption is that the individuals in each group are homogeneous. However, heterogeneity is one of the main features of real populations. Individuals are different in various aspects, in particular regarding their pattern of interactions with other individuals. Indeed, each individual has a finite set of contacts and infection pass trough these contact. Therefore, one needs to integrate the spreading at the individual level in the contact network in order to compute the epidemic dynamics at the population level.

Meta-population models are a convenient framework allowing to relax the homogeneous mixing hypothesis at the sub-population level. However, they are not appropriate to represent the extraordinary complexity of the connectivity pattern of individuals. It is essential to integrate the contact network topology in the epidemic model in order to get a clear idea of the epidemic process. Furthermore, it allows to design control strategies such as contact tracing that can be very helpful at the beginning of the epidemic. Advances in complex networks begin the new era of research for epidemic dynamics in heterogeneous populations. It is the starting point of a great number of studies related to direct route disease [19], [44], [45]. Various network models are used by researchers to account for different underlying patterns. For example, many emerging phenomena in social and biological networks are explained using the theory of complex networks [20]. Considering the network structure allows to capture at the individual level the complex patterns of the epidemics in the human population. The reader can refer to the reviews [46], [47] to get a good idea of the vast research activity on the subject. In the following, other recent and/or influential works are recalled.

Vespignani study the behavior of the epidemic model considering scale-free networks. He analyze real data set of computer virus infections and investigate the meantime of

the existence of viral infection on the Internet in the absence of the epidemic threshold [48] . Mendiola *et al.* present and analyze a SIS model on coupled interconnected complex networks. They use a heterogeneous mean-field approach to find under which condition the endemic state exists. They show that adding links between the two networks can lead to an endemic state in the overall network even if each network taken separately is below its epidemic threshold [49]. Hong *et al.* propose an epidemiological model by exploring the mobility of nodes in a dynamical network. Heterogeneity is caused by the movement of nodes. It affects the propagation dynamics of disease [50]. Castellano *et al.* study the effect of the threshold for epidemic spreading in contact network considering heterogeneity [51]. They show that in the SIS model the power-law degree distribution of the contact network has no crucial effect on the epidemic threshold while this is not the case for the SIR model. Li *et al.* propose an epidemic model based on a synthetic mobility model and a resistance factor that account for the heterogeneity of the individuals. They investigate the influence of nonlinear incidence rate and time delay in the SIR epidemic model, and elaborate the dependence of the basic reproduction number (R_0) on both parameters [52]. Arquam *et al.* propose a delayed SIR model that consider the delay in the infection process. They derive the critical threshold of infection using various underlying network structure [53]. Huang *et al.* present a modified SIS epidemic model that incorporate the individuals heterogeneous contact network patterns. Furthermore, rather than using a constant infection rate for all the population, they propose to relate it to the number of infected in the individual neighborhood. Results of their analysis show that the final number of infected nodes is quite dependant of the heterogeneous infection rate. They establish a relationship between the immunization rate and the recovery rate. They also evaluate various immunization strategies [54]. Hosseini *et al.* present a SEIRS-QV model for malware propagation in an heterogeneous network considering vaccination and quarantine methods. They derive the basic reproductive ratio considering user awareness, network delay and diverse configuration of nodes. They establish the stability conditions to reduce the malware propagation speed [55]. Zhou *et al.* study the continuous-time epidemic model using a SIS model. The authors use edge weights to differentiate the interactions. They derive the epidemic size for a scale-free network and Erdos-Renyi (ER) network. They suggest that the weights play an important role on the epidemic outbreak, and that the final epidemic size is quite variable according to the network topology [56].

III. MODEL DESCRIPTION AND FORMULATION

A block diagram illustrating the vector-host interactions as well as the host to host interactions in the *Seasonal SIR* model is given in Fig. 1. A healthy host may be infected by both routes: 1) a bite by an infected vector, 2) a direct interaction with an infected host. An infected host may transmit the infection to a susceptible vector that bites him. The populations density and dynamics are quite different. The vector population is much larger than the host population, and its lifespan is much shorter. For the sake of simplicity, we do not consider the demography of the vector and host populations during the epidemic process.

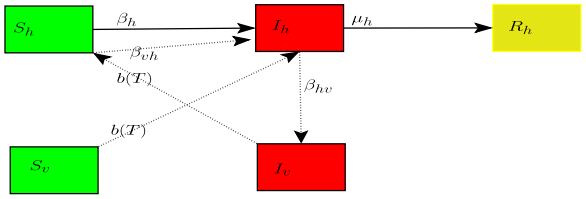

FIGURE 1. Block diagram of the Seasonal SIR model. The host population (top) is split into 3 states: Susceptible S_h,Infectious I_h, and recovered R_h. The vector population (bottom) is split into 2 states: Susceptible S_v and Infectious I_v. Solid arrows indicate the direction individuals can move between states and dashed arrows indicate the direction of transmission. Relevant parameters are the vector biting rate which is temperature dependent $b(T)$, the spreading rate from vector to host β_{vh}, the spreading rate from host to vector β_{hv}, the spreading rate from host to host β_h, and the recovery rate of infected hosts μ_h.

To define the Seasonal SIR model, the following points are assumed.

- N_h represents the size of the host population. It is constant and subdivided into three groups: Susceptible $S_{h_k}(t)$, Infected $I_{h_k}(t)$, and Recovered $R_{h_k}(t)$ of degree k at time t.
- N_v represents the size of the vector population. It is constant and divided into two groups: Susceptible S_v, and Infected I_v. The recovered group is not considered in the vector population due to their short lifespan.
- An infected vector may bite and infect a susceptible host with a rate of $\beta_{vh}b(T)$ where β_{vh} is the spreading rate from vector to host, and $b(T)$ is the biting rate of vectors which is a function of temperature T.
- An infected host, may propagate the disease to a susceptible vector that bites him with a rate $\beta_{hv}b(T)$ where β_{hv} is the spreading rate from host to vector.
- The recovery rate of infected hosts is μ_h
- An infected host can spread the disease to a susceptible host at the rate of β_h.

Note that this model can be used for dual-route disease transmission as well as only vector transmitted disease by setting the transmission rate between hosts β_h at zero.

A. MATHEMATICAL FORMULATION OF THE SEASONAL SIR MODEL

Lets consider a contact network G of size N_h where the nodes represent the host population and the set of links between the hosts is represented by E.

The total host population N_h is divided into Susceptible ($S_{h_k}(t)$), Infected ($I_{h_k}(t)$) and Recovered ($R_{h_k}(t)$) nodes at time t with degree k in such a way that $S_{h_k}(t) + I_{h_k}(t) + R_{h_k}(t) = 1$.

Assume $p(k)$ is the degree distribution of the network, where $k \in [1, N-1]$. The infection and recovery rates of the

host population are represented by β_h and μ_h respectively. β_h and μ_h are $\in [0, 1]$.

Suppose the vector population size is N_v and the fraction of the Susceptible and Infected vectors are $S_v(t)$ and $I_v(t)$ respectively at time t. The vector-borne diseases propagate among hosts by direct contact. It spreads also between the two populations through vectors biting of susceptible or infected hosts.

The transition rules from one state to another are as follows:

- An infected host may propagates the infection directly to a susceptible host by direct contact or indirectly by transmitting it to a susceptible vector that bite him.
- A contaminated vector may spread the infection to a susceptible host when biting him.
- The vector population is sensitive to temperature variations. This dependency is expressed trough the biting rate.
- The recovery process of a host is spontaneous, it does not require any contact. We consider that the recovery rate $\mu_h = 1$ in the following.
- A recovered node can never be infected again.
- Demography is not considered for host and vector populations. The total population of hosts and vectors are constant throughout the epidemic process.

Temperature drives the disease transmission trough various traits of the vector population such as reproduction, development, lifespan and biting rate. It is now well established that between lower and upper temperature limits, the transmission increases until an maximum value and then decreases. Furthermore, extensive empirical and theoretical work has established that most physiological and life history traits respond nonlinearly to temperature – increasing from zero at a thermal minimum approximately up to an optimum before declining back to zero at a thermal maximum. This hump-shaped relationship is nearly universal across measured responses from ectotherm taxa and traits and is predicted from first principles of enzyme kinetic and physiology [57]–[59].

Based on recent studies on the ecology of various vector population [22], [60], [61], we adopt a Gaussian behavior to model the variation of the biting rate with the temperature. It is expressed as follows:

$$b(T) = b_0 e^{-C(T-T_0)^2} \tag{1}$$

where C is constant and b_0 is the maximum biting rate at temperature T_0. The maximum temperature value T_0 varies geographically and across the various vector populations. In tropical or sub-tropical regions, T_0 evolves between $23°C$ and $32°C$.

B. TEMPERATURE DEPENDENT EPIDEMIC SPREADING OVER HETEROGENEOUS NETWORK

We adopt a non-homogeneous mean-field approach in order to integrate the heterogeneity of the host population and the temperature dependence. Considering the above mentioned transitions we get:

TABLE 1. List of the parameters used in the Seasonal SIR model with their description.

Name of Parameter	Interpretation
S_{h_k}	Fraction of healthy hosts of degree k
I_{h_k}	Fraction of contaminated hosts of degree k
R_{h_k}	Fraction of recovered hosts of degree k
$p(k)$	Probability of a node with degree k
S_v	Fraction of healthy vectors
I_v	Fraction of contaminated vectors
β_h	Infection incidence rate from host to host
β_{vh}	Infection incidence rate from vector to host
β_{hv}	Infection incidence rate from host to vector
$b(T)$	Temperature dependent Biting rate of vector
μ_h	Recovery rate of an host

$$\begin{aligned}\frac{dS_{h_k}(t)}{dt} &= -\beta_h k S_{h_k}(t)\Omega_{k_h}(t) \\ &\quad -\beta_{vh} b(T) S_{h_k}(t) I_v(t) \qquad (2)\\ \frac{dI_{h_k}(t)}{dt} &= \beta_h k S_{h_k}(t)\Omega_{k_h}(t) \\ &\quad +\beta_{vh} b(T) S_{h_k}(t) I_v(t) - I_{h_k}(t) \qquad (3)\\ \frac{dR_{h_k}(t)}{dt} &= I_{h_k}(t). \qquad (4)\\ \frac{dS_v(t)}{dt} &= -\beta_{hv} b(T) S_v(t) I_{h_k}(t) - \mu_v S_v(t) \qquad (5)\\ \frac{dI_v(t)}{dt} &= \beta_{hv} b(T) S_v(t) I_{h_k}(t) - \mu_v I_v(t) \qquad (6)\end{aligned}$$

where, $\Omega_{k_h}(t)$ is the coupling function. It contains the probability of a link between a susceptible node of degree k and an infected node at time t.

$$\Omega_{k_h}(t) = \sum_{k=1}^{k_{max}} P(k'|k) I_{h_k}(t) \tag{7}$$

where $P(k'|k)$ is the degree-degree correlation.

For an heterogeneous network it is given by $P(k'|k) = \frac{k' p(k')}{\langle k \rangle}$ [44]. k' is the number of infected nodes connected with a node of degree k

All the variables used in Eqs. ((2) - (6)) are defined in Table 1.

An epidemic occurs if the number of infected vectors increases, i.e., $\frac{dI_v(t)}{dt} > 0$, Hence, from equation 6,

$$\begin{aligned}\frac{dI_v(t)}{dt} &> 0\\ \beta_{hv} b(T) S_v(t) I_{h_k}(t) - \mu_v I_v(t) &> 0\\ \beta_{hv} b(T) S_v(t) I_{h_k}(t) &> \mu_v I_v(t)\\ \frac{\beta_{hv} b(T) S_v(t) I_{h_k}(t)}{\mu_v} &> I_v(t)\end{aligned}$$

At the outset of an epidemic, $S_v(t) \approx 1$ so that,

$$\beta_{hv} b(T) I_{h_k}(t) > I_v(t) \tag{8}$$

The basic reproduction number of the vector population is given by

$$R_{0_v} = \beta_{hv} b(T) I_{h_k}(0) \tag{9}$$

Reporting the left side of equation 8 into Eq. (2) and (3), we get

$$\frac{dS_{h_k}(t)}{dt} = -\beta_h k S_{h_k}(t)\Omega_{k_h}(t) - \beta_{vh} b(T)^2 S_{h_k}(t)\beta_{hv} I_{h_k}(t) \quad (10)$$

$$\frac{dI_{h_k}(t)}{dt} = \beta_h k S_{h_k}(t)\Omega_{k_h}(t) + \beta_{vh} b(T)^2 S_{h_k}(t)\beta_{hv} I_{h_k}(t) - I_{h_k}(t) \quad (11)$$

Combining Eqs. (10) and (4) we get,

$$\frac{dS_{h_k}(t)}{dR_{h_k}(t)} = \frac{-\beta_h k S_{k_h}(t)\sum_{k=1}^{k_{max}} P(k'|k) I_{h_k}(t)}{I_{h_k}(t)} + \frac{\beta_{vh} b(T) S_{h_k}(t)\{\beta_{hv} b(T) I_{h_k}(t)\}}{I_{h_k}(t)}. \quad (12)$$

Integrating both side,

$$S_{h_k}(t) = e^{-\beta_h k \sum_{k=1}^{k_{max}} P(k'|k) R_{h_k}(t) + \beta_{vh} b(T)\{\beta_{hv} b(T)\} R_{h_k}(t)}$$

Assume,

$$\sum_{k=1}^{k_{max}} P(k'|k) R_{h_k}(t) = \theta_{h_k}(t) \quad (13)$$

At $t \to \infty$, the epidemic reaches a steady state hence, $I_{h_k}(\infty) = 0$. Therefore,

$$S_{h_k}(\infty) = 1 - I_{h_k}(\infty) - R_{h_k}(\infty) \quad (14)$$

$$S_{h_k}(\infty) = e^{-\beta_h k \theta_{h_k}(\infty) + \beta_{vh} b(T)^2 \beta_{hv} R_{h_k}(\infty)}$$

$$R_{h_k}(\infty) = 1 - e^{-\beta_h k \theta_{h_k}(\infty) + \beta_{vh} b(T)^2 \beta_{hv} R_{h_k}(\infty)} \quad (15)$$

Now, assume $f(R_{h_k}(\infty))$ as a function of $R_{h_k}(\infty)$ is strictly increasing. If we put $R_{h_k}(\infty) = 0$, then the total population of host recover and it gives us a very common solution with no significance. It also describes that the system is in the disease free state.

Therefore, we have to find a solution which lies between 0 and 1. But, we cannot express Eq. (15) in term of $R_{h_k}(\infty)$ as it is coupled with the network parameters. Therefore, we need to solve it using Eq. (13),

$$\theta_{h_k}(t) = \sum_{k=1}^{k_{max}} P(k'|k) R_{h_k}(t)$$

$$\theta_{h_k}(\infty) = \sum_{k=1}^{k_{max}} P(k'|k) R_{h_k}(\infty) \quad (16)$$

$$\theta_{h_k}(\infty) = \sum_{k=1}^{k_{max}} P(k'|k) \times \left[1 - e^{-\beta_h k \theta_{h_k}(\infty) + \beta_{vh} b(T)^2 \beta_{hv} R_{h_k}(\infty)}\right] \quad (17)$$

$$\frac{df(\theta_{h_k}(\infty))}{d\theta_{h_k}(\infty)}\Big|_{\theta_{h_k}(\infty)=0} > 1 \quad (18)$$

Putting the right side of equation (17) in equation (18) and derivating by $\theta_{h_k}(\infty)$, we get

$$\sum_{k=1}^{k_{max}} P(k'|k)(\beta_h k + \beta_{vh} b(T)^2 \beta_{hv} \frac{dR_{h_k}(\infty)}{d\theta_{h_k}(\infty)}) \times e^{-\beta_h k \theta_{h_k}(\infty) - \beta_{vh} b(T)^2 \beta_{hv} R_{h_k}(\infty)}\Big|_{\theta_{h_k}(\infty)=0} > 1 \quad (19)$$

$$\frac{dR_{h_k}(\infty)}{d\theta_{h_k}(\infty)} = \frac{\frac{dR_{h_k}(\infty)}{dR_{h_k}(\infty)}}{\frac{d\theta_{h_k}(\infty)}{dR_{h_k}(\infty)}}$$

$$\frac{dR_{h_k}(\infty)}{d\theta_{h_k}(\infty)} = \frac{1}{\sum_{k=1}^{k_{max}} P(k'|k)} \quad (20)$$

Reporting the value of Eq. (20) into the above Eq. (18),

$$\frac{df(\theta_{h_k}(\infty))}{d\theta_{h_k}(\infty)}\Big|_{\theta_{h_k}(\infty)=0} > 1$$

$$\sum_{k=1}^{k_{max}} P(k'|k)\beta_h k + \beta_{vh} b(T)^2 \beta_{hv} > 1 \quad (21)$$

Reporting $\sum_{k=1}^{k_{max}} P(k'|k) = \frac{\sum_{k=1}^{k_{max}} kp(k)}{\langle k \rangle}$ in Eq. (21)

$$\frac{\sum_{k=1}^{k_{max}} kp(k)}{\langle k \rangle}\beta_h k + \beta_{vh} b(T)^2 \beta_{hv} > 1$$

$$\frac{\langle k^2 \rangle}{\langle k \rangle}\beta_h + \beta_{vh} b(T)^2 \beta_{hv} > 1 \quad (22)$$

The left side of the Eq. (22) is the basic reproduction number R_{0_h}.

$$R_{0_h} = \frac{\langle k^2 \rangle}{\langle k \rangle}\beta_h + \beta_{vh} b(T)^2 \beta_{hv} \quad (23)$$

where β_h, β_{vh} and β_{hv} are constant characterizing the disease, and $\frac{\langle k^2 \rangle}{\langle k \rangle}$ is a constant characterizing the contact network statistics.

Indeed, $\langle k^2 \rangle$ is the second moment and $\langle k \rangle$ is the first moment of the degree distribution of the contact network. Therefore, for a given network, R_{0_h} is proportional to the square of the biting rate i.e. $b(T)^2$.

For an homogeneous network [14], the basic reproduction number is given by:

$$R_{0_h} = (\beta_h \langle k \rangle + \beta_{vh} b(T)^2 \beta_{hv}) \quad (24)$$

IV. RESULTS AND ANALYSIS

In this section simulations are performed based on the non-homogeneous mean field derivation. The simulation setup is given, and the results of the simulations are discussed. The B-A Model is used as the underlying contact network in order to evaluate the proposed *Seasonal SIR* model. The values of the various parameters used in the simulations are reported in Table 2. They have been chosen on the basis of the literature survey.

Our primary goal is to analyze the impact of the temperature on the epidemic process in the heterogeneous host

TABLE 2. Values of the parameters values used in the simulations.

Name of Parameter	Value
Number of nodes for host population	2000
Number of edges to attach for BA model(m)	10
Vector population size	100000
Initial Number of infected host	1
Initial Number of infected vector	100
Host Recovery Rate (μ_h)	1
T_0	$25°C$
Biting rate of vector (b_0) at T_0	0.4
C	0.008

population as well as the vector population. In the simulations, we choose to use a temperature range between $4.3°C$ to $37°C$ because a vast majority of vector species live in this temperature range. Beyond this range, the vector population vanishes and the biting rate is equal to zero [26]. In case one wants to tailor the experiments to a specific vector-borne disease, temperature range must be adapted. To see the impact of transmission rate on evolution of the epidemic spreading, we choose the value of various transmission rate, β_h, β_{vh} and β_{hv} from 0.1 to 0.9, as we do not focus on a specific vector-borne disease. There are many ways to introduce heterogeneity in the interactions of the host population. We choose to use the Barabasi - Albert model for the simulations, as it is the most influential model that allows accounting for heterogeneity in the complex network literature [20], [21], [62], [63].

A. EPIDEMIC SPREADING IN AN HETEROGENEOUS NETWORK

The disease spreading dynamics with the *Seasonal SIR* Model based on an heterogeneous contact network topology (B-A model) is shown in Figure 2. The simulations are performed considering a temperature range from $4.3°C$ to $37°C$ in order to assess the impact of temperature variations. As the vector population is coupled with the host population trough biting, it leads to the seasonal disease spreading depending upon the environmental condition. Epidemic spreading in the host population increases with the increase of vector biting. Such type of seasonal disease exists until the extinction of the vector population. Susceptible population decreases to 0 at 9 time steps. The size of the infectious population grows until it reaches 0.79 of the population quite quickly, then it decreases slowly. This process is completed after 70 time steps when the whole host population recover. Note that time steps need to be converted in real time units according to the disease under consideration.

Figure 3 represents the Seasonal SIR model dynamics when there is a single route of transmission. In this case, infections are only due to interactions between the hosts. We use the same set of parameters used in the previous experiment for comparative purposes. The model reduces in this case to the classical SIR model. One can notice that the proportion of infected individuals is lower and that the

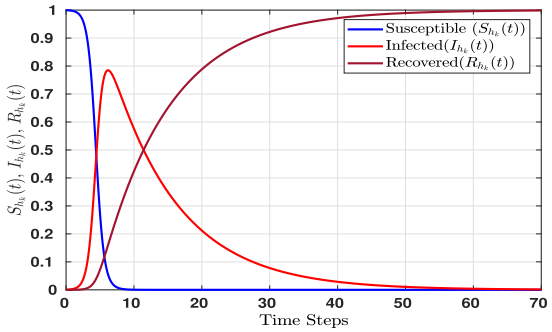

FIGURE 2. Evolution of the epidemic spreading considering both routes of transmission. The contact network of the host population follows the B-A model with $m = 10$. The transmission rate values are $\beta_h = 0.6$, $\beta_{vh} = 0.4$ and $\beta_{hv} = 0.6$. The seasonal biting rate parameters are $b_0 = 0.4$, $T_0 = 25°C$ and $C = 0.008$.

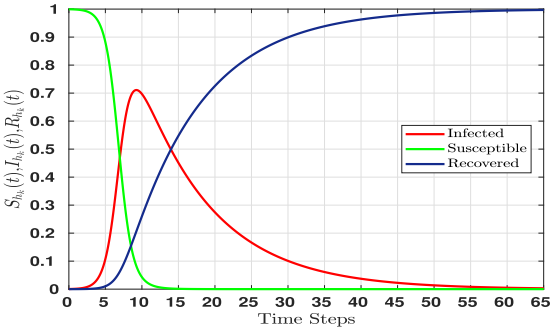

FIGURE 3. Evolution of the epidemic spreading considering a single route of transmission (host to host). The contact network of the host population follows the B-A model with $m = 10$. The transmission rate values are $\beta_h = 0.6$, $\beta_{vh} = 0$ and $\beta_{hv} = 0$.

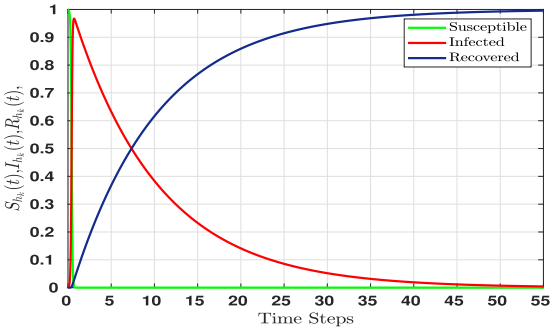

FIGURE 4. Evolution of the epidemic spreading in an heterogeneous host population. the contact network follows the B-A model with $m = 10$. The transmission rate values are $\beta_h = 0.6$, $\beta_{vh} = 0.4$ and $\beta_{hv} = 0.6$. The biting rate parameter does not depend on temperature $b_0 = 0.4$.

duration of the epidemics is shorter as compared to the two routes case. Susceptible population decreases to 0 at 13 time steps. Indeed, with both vectors and hosts, the infection peak at 0.79 and get extinct after 70 time steps, while without vector transmission, the peak value is 0.704 and the disease last after 65 time steps. As expected, the epidemic reaches more people and last longer when there is two routes of transmissions rather than with a single route.

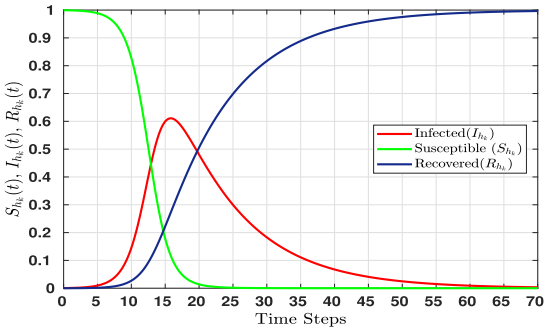

FIGURE 5. Evolution of the epidemic spreading in an homogeneous host population. The contact network follows the Watts-Strogatz Model with $p = 0.2$ and $k = 30$. The transmission rate values are $\beta_h = 0.6$, $\beta_{vh} = 0.4$ and $\beta_{hv} = 0.6$. The seasonal biting rate parameters are $b_0 = 0.4$, $T_0 = 25°C$ and $C = 0.008$.

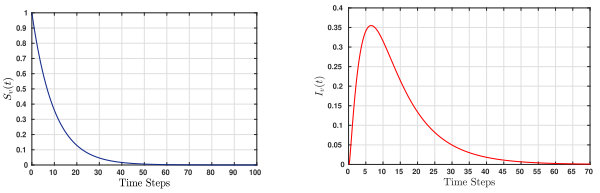

(a) Susceptible Vector (b) Infected Vector

FIGURE 6. Evolution of the epidemic spreading in the vector population. The transmission rate values are $\beta_h = 0.6$, $\beta_{vh} = 0.4$ and $\beta_{hv} = 0.6$. The seasonal biting rate parameters values are $T_0 = 25°C$, $b_0 = 0.4$ and $C = 0.008$.

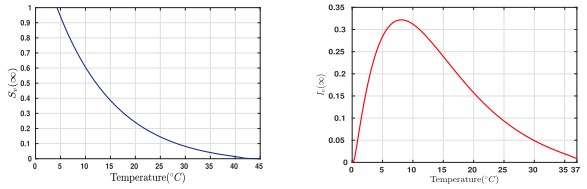

(a) Susceptible Vector (b) Infected Vector

FIGURE 7. Evolution of the epidemic spreading in the vector population versus the temperature. The transmission rate values are $\beta_h = 0.6$, $\beta_{vh} = 0.4$ and $\beta_{hv} = 0.6$. The seasonal biting rate parameters are $b_0 = 0.4$ at $T_0 = 25°C$ and $C = 0.008$.

Figure 4 represents the epidemic spreading in the host population with the same set of parameters used in the previous simulations. The only difference is that in this case the biting rate is not dependant of the temperature. It has the same constant value $b_0 = 0.4$. One can see that the infection propagates immediately to a maximum and then it decreases monotonically during 55 time steps. Additionally the proportion of infected hosts is much higher with a maximum number of 0.99 of the population infected as compared to 0.79 with the Seasonal SIR model. The main lesson learned so far is that neglecting to take into account the temperature influence in the epidemic dynamics can lead to overestimating the proportion of the population that can be infected and the transmission speed of the disease.

Figure 5 represents the epidemic spreading in the host population in the same conditions than in the previous experiments. The difference lies in the topology of the contact network. While in results reported in Figure 2 the B-A model is used,in this case, the contact network is homogeneous (Watts & Strogatz model). It appears that the topology of the contact network affects both the peak value of the fraction of infected host I_{h_m} and the time to reach this value t_m. Indeed, the peak value is 0.79 for the heterogeneous network as compared to 0.61 for the homogeneous network. This value is reached two times earlier in the heterogeneous network. So, one can conclude that using an homogeneous contact network hypothesis instead of a more realistic topology, can lead to an underestimation of the proportion of the infected population and also of the speed of the disease spreading. This result is quite important, as it may guide the decision process in order to design efficient control strategies in real situations.

The epidemic dynamics in the vector population with the temperature dependence is shown in Fig. 6(a)&(b). The fraction of infected vectors increases until it reaches a maximum value of 0.35 after a few time steps, then it decreases monotonically. The epidemic persists until there is no more susceptible in the vector population, as shown in Figure 6(b).

The evolution of the proportion of susceptible and infected vectors while varying the temperature is plotted in Fig.7(a)&(b) respectively. One can see that after $37°C$, the vector population vanishes. It is highly infected in the temperature range between $5°C$ to $30°C$. These results are in line with findings reported in the literature. Indeed, According to [64], [65], the vector population is highly dependent on the local temperature and especially after the rainy season. During this period, the size of the vector population increases. In tropical and sub-tropical regions when the temperature increases above $37°C$, the vector population vanishes.

The impact of temperature variations on the infection dynamics in the host population is shown in Fig. 8. An infected vector can bite multiple hosts causing the infection in the host population. The infection in the host population propagates much faster than in the vector population because the host population is infected both by host to host interactions as well as vector to host interactions. As the temperature increases, the biting rate decreases and the infection in the host population also vanishes.

The effect of temperature variations on the infection dynamics in the host population with single route transmission (vector to human) is shown in Fig. 9. The infection in the host population is only due to vector to host interactions. As the temperature increases, infection increase to a maximum value at $25°C$. After that the biting rate and the infection in the host population decreases with the temperature untill it vanishes.

The effect of temperature variations on the infection dynamics in the vector population with single transmission route (vector to human) is shown in Fig. 10. The infection in the vector population is transmitted due to biting of vector to host. Therefore the human to human transmission rate β_h is

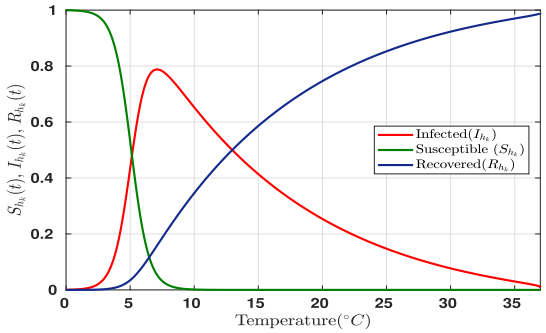

FIGURE 8. Evolution of the epidemic spreading in the heterogeneous host population versus the temperature. The contact network follows the B-A model with $m = 10$. The transmission rate values are $\beta_h = 0.6$, $\beta_{vh} = 0.4$ and $\beta_{hv} = 0.6$. The seasonal biting rate parameters are $b_0 = 0.4$ at $T_0 = 25°C$ and $C = 0.008$.

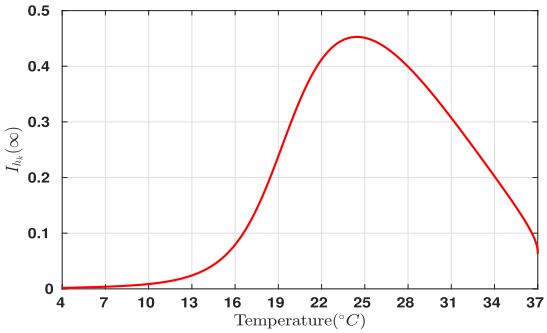

FIGURE 9. Evolution of the epidemic spreading in the host population versus the temperature using a single transmission route (vector to human). The transmission rate values are $\beta_h = 0$, $\beta_{vh} = 0.4$ and $\beta_{hv} = 0.6$. The seasonal biting rate parameters are $b_0 = 0.4$ at $T_0 = 25°C$ and $C = 0.008$.

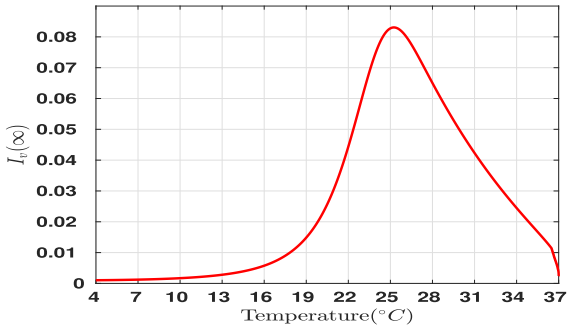

FIGURE 10. Evolution of the epidemic spreading in the vector population versus the temperature using a single transmission route (vector to human). The transmission rate values are $\beta_h = 0$, $\beta_{vh} = 0.4$ and $\beta_{hv} = 0.6$. The seasonal biting rate parameters are $b_0 = 0.4$ at $T_0 = 25°C$ and $C = 0.008$.

equal to zero. As the temperature increases, the infection in the vector population also increase to a maximum at $25°C$. Then for higher temperature values, the biting rate and the infection in the vector population decreases untill it vanishes at $37°C$.

B. INFLUENCE OF THE TRANSMISSION RATES ON THE EPIDEMIC DYNAMICS

In order to investigate the impact of the various spreading rates on the epidemic dynamics, we perform a number of

TABLE 3. Influence of the host to host transmission rate β_h on the maximum proportion of infected individuals in the host population I_{hm} at time t_m. The contact network follows the B-A model with $m = 10$. The other transmission rate values are $\beta_{hv} = 0.5$ and $\beta_{vh} = 0.4$. The seasonal biting rate parameters are $b_0 = 0.4$ at $T_0 = 25°C$ and $C = 0.008$.

β_h	0.1	0.2	0.3	0.4	0.5	0.6	0.7	0.8	0.9
I_{h_m}	0.63	0.72	0.76	0.77	0.81	0.83	0.85	0.86	0.88
t_m	14	9	7	6	5	4	4	3	3

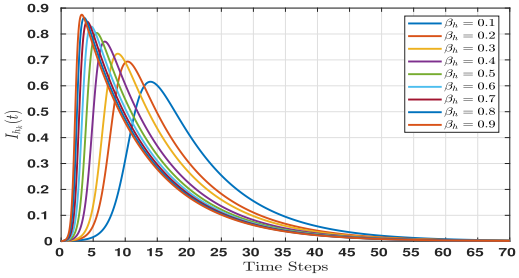

FIGURE 11. Evolution of the epidemic spreading in an heterogeneous host population for various values of the host to host transmission rate β_h . The contact network follows the B-A model with $m = 10$. The other transmission rate values are $\beta_{vh} = 0.4$ and $\beta_{hv} = 0.5$. The seasonal biting rate parameters are $b_0 = 0.4$ at $T_0 = 25°C$ and $C = 0.008$.

simulations with different values of β_h, β_{vh}, β_{hv}. First of all, we consider the influence of the transmission parameters separately, then we investigate their combination.

Fig. 11 illustrates the effect of variation of the host to host transmission rate parameter β_h on the fraction of infected host population. All the curves exhibit the same behavior. The proportion of infected host increases rapidly to a maximum value I_{h_m} and then it decreases slowly until there is no more infected host. As the value of β_h increases, the epidemic spreads much faster in the host population. The value of the maximum proportion of infected individuals I_{h_m} at time t_m in the host population with β_h varying in the range 0.1 to 0.9 is given in Table 3.

One can see in Table 3 that increasing the value of β_h increases the peak of infection I_{h_m} in the host population, and that this value is reached sooner. However, it does not affect the disease duration that last around 65 time steps.

The values of β_h have little effects on the epidemic dynamics in the vector population as compared to host population as shown in Fig. 12. Increasing β_h does not change too much the value of the maximum fraction of infected vectors I_{v_m}. Variations of β_h is directly affecting the proportion of infected hosts, while it has less impact in the infection spreading in the vector population. Values of the maximum proportion of infected vector I_{v_m} and associated time t_m while varying the transmission rate in the host population β_h in the range 0.1 to 0.9 are reported in Table 4. One can see that the variations are much more smaller as compared to the variations in the host population.

In order to investigate the influence of the vector to host transmission rate in the epidemic dynamics independently of the host to host interaction, the value of β_{vh} is increased

TABLE 4. Influence of the host to host transmission rate β_h on the maximum proportion of infected individuals in the vector population I_{v_m} at time t_m. The contact network follows the B-A model with $m = 10$. The other transmission rate values are $\beta_{hv} = 0.5$ and $\beta_{vh} = 0.4$. The seasonal biting rate parameters are $b_0 = 0.4$ at $T_0 = 25°C$ and $C = 0.008$.

β_h	0.1	0.2	0.3	0.4	0.5	0.6	0.7	0.8	0.9
I_{v_m}	0.28	0.30	0.31	0.31	0.32	0.32	0.32	0.32	0.33
t_m	9	8	7	7	7	6	6	6	6

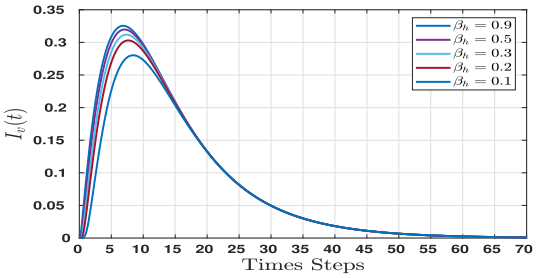

FIGURE 12. Evolution of the epidemic spreading in the vector population for various values of the host to host transmission rate β_h. The contact network follows the B-A model with $m = 10$. The other transmission rate values are $\beta_{vh} = 0.4$ and $\beta_{hv} = 0.5$. The seasonal biting rate parameters are $b_0 = 0.4$ at $T_0 = 25°C$ and $C = 0.008$.

TABLE 5. Influence of the vector to host transmission rate $\beta_v h$ on the maximum proportion of infected individuals in the host population I_{h_m} at time t_m. The contact network follows the B-A model with $m = 10$. The other transmission rate values are $\beta_h = 0$ and $\beta_{vh} = 0.4$. The seasonal biting rate parameters are $b_0 = 0.4$ at $T_0 = 25°C$ and $C = 0.008$.

β_{vh}	0.1	0.2	0.3	0.4	0.5	0.6	0.7	0.8	0.9
I_{h_m}	0.17	0.31	0.39	0.45	0.49	0.52	0.54	0.56	0.58
t_m	44	37	32	29	27	26	25	24	23

linearly in the range 0.1 to 0.9 with a step of 0.1 while keeping $\beta_h = 0$. The evolution of the infected fraction in the host population versus time for the various values of the β_{vh} parameter are reported in Figure 13. All the curves exhibit the same behavior. As time increases, the proportion of infected hosts increases until a maximum value, and then it decreases until there is no more host infected. However, both the max proportion of infected hosts I_{h_m} and the time t_m needed to reach this value are impacted by the variations of β_{vh}. Table 5 reports the values of I_{h_m} and t_m to illustrate this behavior.

One can notice that as β_{vh} increases, the max proportion of infected host I_{h_m} increases. However the time needed to reach this maximum value decreases. The higher the value of β_{vh}, the higher the proportion of infected and the sooner this proportion is reached.

Variations of the vector to host transmission rate β_{vh} also affect the epidemic spreading behavior in the vector population. Figure 14 reports the results of the vector population dynamics versus time while varying β_{vh} from 0.1 to 0.9 with a step of 0.1 and keeping $\beta_h = 0$. The overall behavior is quite similar to the one observed in the host population. As β_{vh} increases, the maximum fraction of infected vectors I_{v_m} increases and this value is reached sooner. Note however that the vector population is impacted to a lesser extent as

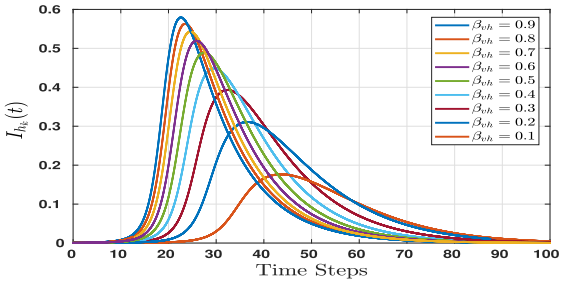

FIGURE 13. Evolution of the epidemic spreading in an heterogeneous host population for various values of the vector to host transmission rate β_{vh}. The contact network follows the B-A model with $m = 10$. The other transmission rate values are $\beta_h = 0$ and $\beta_{hv} = 0.5$. The seasonal biting rate parameters are $b_0 = 0.4$ at $T_0 = 25°C$ and $C = 0.008$.

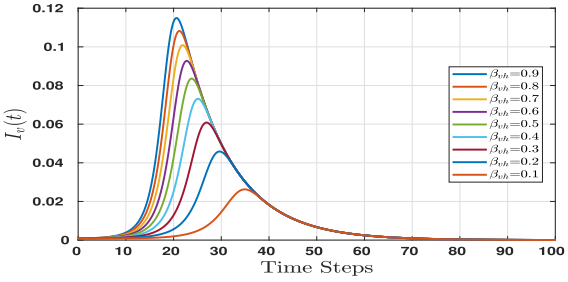

FIGURE 14. Evolution of the epidemic spreading in the vector population for various value of the vector to host transmission rate β_{vh}. The contact network follows the B-A model with $m = 10$. The other transmission rate values are $\beta_h = 0$ and $\beta_{hv} = 0.5$. The seasonal biting rate parameters are $b_0 = 0.4$ at $T_0 = 25°C$ and $C = 0.008$.

TABLE 6. Influence of the vector to host transmission rate $\beta_v h$ on the maximum proportion of infected individuals in the vector population I_{v_m} at time t_m. The contact network follows the B-A model with $m = 10$. The other transmission rate values are $\beta_h = 0$ and $\beta_{vh} = 0.4$. The seasonal biting rate parameters are $b_0 = 0.4$ at $T_0 = 25°C$ and $C = 0.008$.

β_{vh}	0.1	0.2	0.3	0.4	0.5	0.6	0.7	0.8	0.9
I_{v_m}	0.02	0.04	0.06	0.07	0.08	0.09	0.10	0.11	0.12
t_m	33	29	27	25	24	23	22	21	20

compared to the host population. Table 6 reports the values of I_{v_m} and associated time t_m for various values of β_{vh} to illustrate our findings.

We now turn to the evaluation of the influence of the host to vector transmission rate β_{hv} in the epidemic dynamics. To do so, starting from 0.1, the value of β_{hv} is increased until 0.9 with a step of 0.1 while keeping $\beta_h = 0.4$. As there is no difference between all the curves, we report only the results for $\beta_{hv} = 0.5$ in Figure 15. Modifying the value of β_{hv} does not affect the epidemic spreading in the host population. In other words, β_{hv} has no influence on the epidemic dynamics in the host population. The value of the maximum fraction of infected individuals in the host population I_{h_m} at time t_m does not change whatever the value of β_{hv}. It is around 0.78. Indeed, as β_{hv} measures the transfer rate of the disease from the host to the vector population, it doesn't affect the infection process in the host population directly.

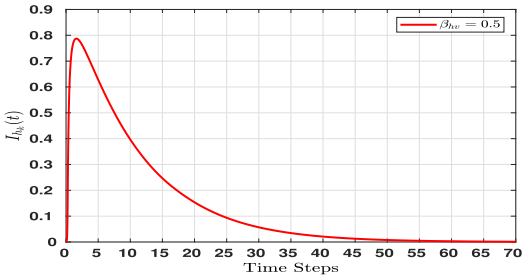

FIGURE 15. Evolution of the epidemic spreading in the host population with the host to vector transmission rate $\beta_{hv} = 0.5$. The contact network follows the BA model with $m = 10$. The other transmission rate values are $\beta_h = 0.4$ and $\beta_{vh} = 0.5$. The seasonal biting rate parameters are $b_0 = 0.4$ at $T_0 = 25°C$ and $C = 0.008$.

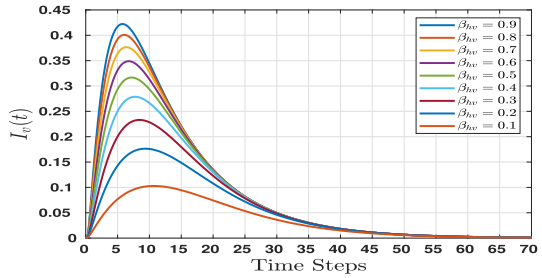

FIGURE 16. Evolution of the epidemic spreading in the vector population for various values of the host to vector transmission rate β_{hv}. The contact network of the host population follows the B-A model with $m = 10$. The other transmission rate values are $\beta_h = 0.4$ and $\beta_{vh} = 0.5$. The seasonal biting rate parameters are $b_0 = 0.4$ at $T_0 = 25°C$ and $C = 0.008$.

TABLE 7. Influence of the host to vector transmission rate $\beta_h v$ on the maximum proportion of infected individuals in the vector population I_{vm} at time t_m. The contact network follows the B-A model with $m = 10$. The other transmission rate values are $\beta_h = 0$ and $\beta_{vh} = 0.5$. The seasonal biting rate parameters are $b_0 = 0.4$ at $T_0 = 25°C$ and $C = 0.008$.

β_{hv}	0.1	0.2	0.3	0.4	0.5	0.6	0.7	0.8	0.9
I_{v_m}	0.10	0.18	0.23	0.27	0.31	0.35	0.38	0.40	0.42
t_m	10	9	8	7	7	6	6	5	5

Now lets evaluate the impact of β_{hv} on the epidemic dynamics in the vector population in the same conditions than above. Results are shown in Figure 16. According to these curves, it is clear that the value of β_{hv} has a huge impact on the epidemic spreading process in the vector population. As β_{hv} increases from 0.1 to 0.9, the value of the peak of infection I_{v_m} increases from 0.10 to 0.42 Furthermore the peak is reached faster. Ten time steps are needed to reach the peak value for $\beta_{vh} = 0.1$, while it is reached in 5 time steps for $\beta_{vh} = 0.9$. Table 7 reports the values of I_{v_m} and the corresponding time t_m for the various values of β_{hv}. It shows that β_{hv} is a quite important parameter in order to evaluate the epidemic spreading in the vector population.

We now evaluate the combined effect of both routes of infection (vector to host and host to host) by varying the transmission rates β_h and β_{vh} simultaneously. Both values are kept equal and vary in the range 0.1 to 0.9 with a step of 0.1. The combined effects of both parameters on the epidemic spreading in the host population is shown in Figure 17. All the curves exhibit a similar behavior. The fraction of infected

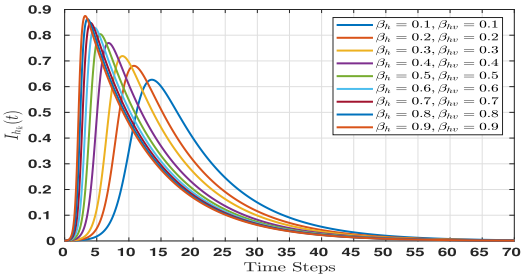

FIGURE 17. Evolution of the epidemic spreading in an heterogeneous host population for various value of the transmission rates β_h and β_{vh}. The contact network follows the B-A model with $m = 10$. The host to vector transmission rate value is $\beta_{hv} = 0.5$. The seasonal biting rate parameters are $b_0 = 0.4$ at $T_0 = 25°C$ and $C = 0.008$.

TABLE 8. Influence of the combination of the host to vector transmission rate β_h and the vector to host transmission rate β_{vh} on the maximum proportion of infected individuals in the host population I_{h_m} at time t_m. The contact network follows the B-A model with $m = 10$. The other transmission rate values are $\beta_h = 0$ and $\beta_{vh} = 0.5$. The seasonal biting rate parameters are $b_0 = 0.4$ at $T_0 = 25°C$ and $C = 0.008$.

β_{vh}	0.1	0.2	0.3	0.4	0.5	0.6	0.7	0.8	0.9
β_h	0.1	0.2	0.3	0.4	0.5	0.6	0.7	0.8	0.9
I_{h_m}	0.62	0.67	0.71	0.74	0.79	0.83	0.84	0.85	0.86
t_m	14	11	9	7	6	5	4	4	3

individuals increases quickly to a maximum value, and then it decreases slowly until all the population recover. The peak value of the epidemic I_{h_m} increases from 0.62 to 0.83 when the values of β_h and β_{vh} increase from 0.1 to 0.6, then we observe a saturation process. Indeed, the value of I_{h_m} is equal to 0.84 for $\beta_h = 0.7$ and $\beta_{vh} = 0.7$. It reaches 0.86 when the values of β_h and β_{vh} are equal to 0.9. Note that as the values of the infection rates increase the peak is reached faster. Table 8 reports the values of I_{h_m} and t_m for the various values of β_h and β_{vh}. While 14 time steps are needed to reach the maximum fraction of infection I_{h_m} for $\beta_h = 0.1$ and $\beta_{vh} = 0.1$, it is reached almost five times earlier when both values are equal to 0.9.

To evaluate the combined effect of β_h and β_{vh} on the epidemic spreading in the vector population, we perform the same simulation process than the one used for the host population. That is to say, the values of β_h and β_{vh} vary simultaneously from 0.1 to 0.9 with a step of 0.1. Results are reported in Figure 18. We observe a similar behavior than for the host population. Indeed, the value of the peak $I_v(max)$ increases from 0.28 to 0.32 when the value of β_h and β_{vh} vary from 0.1 to 0.4. After that, increasing the value of β_h and β_{vh} does not affect the value of the peak I_{v_m} which remains around 0.32. Table 9 report the values of I_{v_m} and t_m for the various values of β_h and β_{vh} to illustrate this behavior. One can see that if the proportion of infected vectors is quite sensitive to this parameters variations, the timing is not so affected as compared to the host population in similar conditions.

However, for comparative purpose, the basic reproduction number R_{0_h} is computed for an homogeneous and non homogeneous contact networks with the same set of parameters. Results listed in Table 10 show that it is greater for the heterogeneous than for the homogeneous topology. Indeed,

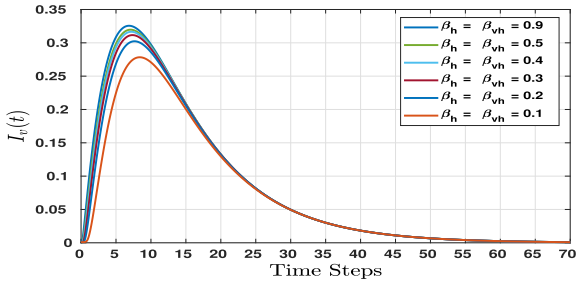

FIGURE 18. Evolution of the epidemic spreading in the vector population for various value of the transmission rates β_h and β_{vh}. The contact network follows the B-A model with $m = 10$. The host to vector transmission rate value is $\beta_{hv} = 0.5$. The seasonal biting rate parameters are $b_0 = 0.4$ at $T_0 = 25°C$ and $C = 0.008$.

TABLE 9. Influence of the combination of the host to vector transmission rate β_h, and the vector to host transmission rate β_{vh} on the maximum proportion of infected individuals in the vector population I_{h_m} at time t_m. The contact network follows the BA model with $m = 10$. The other transmission rate values are $\beta_h = 0$ and $\beta_{vh} = 0.5$. The seasonal biting rate parameters are $b_0 = 0.4$ at $T_0 = 25°C$ and $C = 0.008$.

β_{vH}	0.1	0.2	0.3	0.4	0.5	0.6	0.7	0.8	0.9
β_h	0.1	0.2	0.3	0.4	0.5	0.6	0.7	0.8	0.9
I_{v_m}	0.28	0.30	0.31	0.32	0.32	0.32	0.32	0.32	0.33
t_m	9	8	7	7	7	6	6	6	6

TABLE 10. Effect of the network topology on the basic Reproduction Rate(R_{0_h}) at $T_0 = 25°C$ .The parameter of the B-A model is $m = 10$. The Watts and Strogatz model parameters are $p = 0.2$ and $k = 30$. The transmission rate values are $\beta_h = 0.6$ and $\beta_{hv} = 0.6$ and $\beta_{vh} = 0.4$. The seasonal biting rate parameter $b_0 = 0.4$ at T_0.

Type of Contact Network	R_{0_h}
Heterogeneous Network (B-A Model)	23.1
Homogeneous Network (WS Model)	18.04

TABLE 11. Statistics of diseases.

Disease Name	Number of Infected Host
Malaria	2056
Dengue	453

in heterogeneous networks, high degree nodes are super spreaders, and their high connectivity is a good activator of the epidemics.

C. DISEASE DATASET

In order to evaluate the temperature dependence in real situations, we have collected data from the Hospital of New Delhi for various vector-borne diseases together with environmental conditions. The raw data contains 2509 patients. After refinement of data, the various diseases of interest observed are classified in Table 11.

Although diseases spread all the year round, in summer their impact is very high, as shown in Figure 19. The corresponding average temperature is also plotted in Figure 20. The average temperature of various countries is also plotted in Figure 21, where vector-borne diseases are prominent. Previous models suggests that vector-borne diseases emerge between $12°C$ and $34°C$ [66], [67]. They also suggests that biting is linearly dependent on temperature [67]. Our new model incorporates the influence of temperature in the epidemic process. It is inspired by the dataset of 2 types of diseases, plotted in Fig. 19. These data show that epidemic spreading is greatly affected by temperature variation, especially in the range of $22°C$ to $34°C$. We also observe the severe impact of epidemic spreading after a rainy season especially in India where humidity is high, and the temperature is within a range of $22°C$ to $34°C$.

People are mostly infected between June to October of Malaria, as shown in Figure 19(a). This period is the rainy season in India. During the rainy season, when the temperature is within the range of $22°C$ to $34°C$, Dengue fever spreads quickly between June and December. In September, the cases of Dengue fever are maximum, as shown in Figure 19(b). These data show that the impact of disease spreading is high from June to November. we can see in Figure 20(a) that during these months, the temperature range is favorable for the vector population. Such a situation leads to an increase of biting. Another important environmental parameter that affects the spreading of vector-borne disease is humidity. The average humidity of Delhi-NCR is plotted in Figure 20(b). The humidity between June and December is higher than the other months. Vector-borne diseases show a severe impact within the period of June to December. Lets look at Figure 21 reporting the average monthly temperature recorded in four countries during one year. One can see that except for philippines the curves are unimodal, and that they exhibit a Gaussian shape.

V. CONCLUSION AND FUTURE WORK

In this paper, a seasonal vector-borne disease model, *Seasonal SIR* is proposed and investigated. It combines the impact on the epidemic dynamics of the temperate conditions with the heterogeneous nature of the contact network of the host population. The impact of the temperature is integrated in the model using the biting rate of the vector population. It is defined as a Gaussian function of the temperature. The heterogeneity of the contact network in the host population is incorporated in the model using an heterogeneous mean-field approach. The basic reproduction rate of vector-borne diseases is derived. It is proportional to the square of the biting rate ($b(T)$). Extensive simulations are performed in order to investigate the influence of the temperature and of the heterogeneity of the contact network. To perform the simulations, the B-A model is assumed for the heterogeneous contact network and the Watts & Strogatz model for the homogeneous contact network. Results allow a better interpretation of the complex interplay between the host population, the vector population and the environmental conditions of vector-borne diseases. It appears that failing to integrate the temperature variations in the model can lead to an overestimation of the fraction of infected population and also to an underestimation of the speed of the propagation of the epidemic. In the same line, considering an homogeneous contact network instead of an heterogeneous contact network can lead to a poor appreciation of the epidemic dynamics. Indeed, comparison

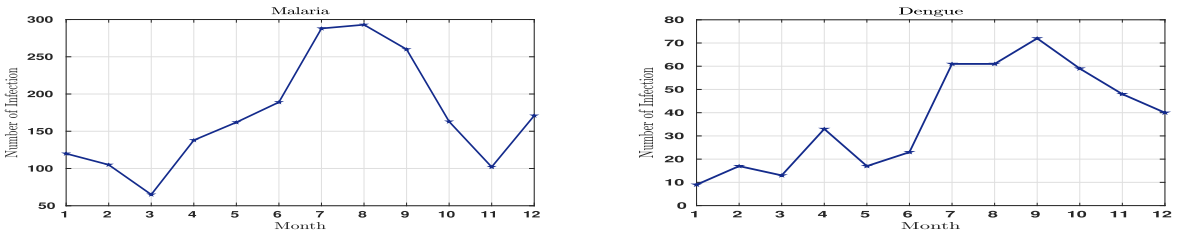

(a) Infection due to Malaria in each month

(b) Infection due to Dengue in each month

FIGURE 19. Evolution of the number of infection during the year for ((a) Malaria, (b) Dengue. Data recorded from the hospital of New Delhi.

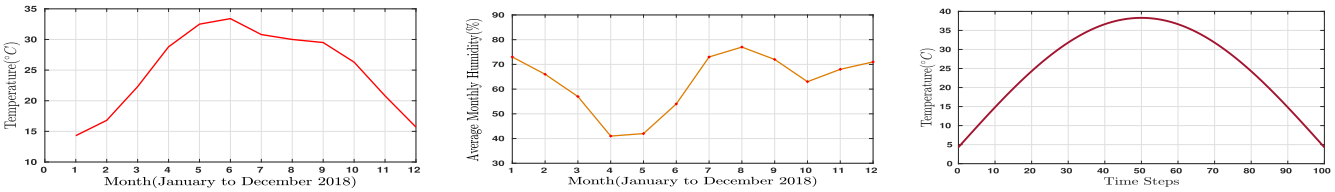

(a) Average Temperature of Delhi-NCR month wise

(b) Average humidity of Delhi-NCR month wise

(c) Synthetic Model of Temperature

FIGURE 20. Average monthly temperatures (a) and humidity (b) recorded in Delhi-NCR during the 2018 civil year. Simulated temperature using a gaussian distribution (c).

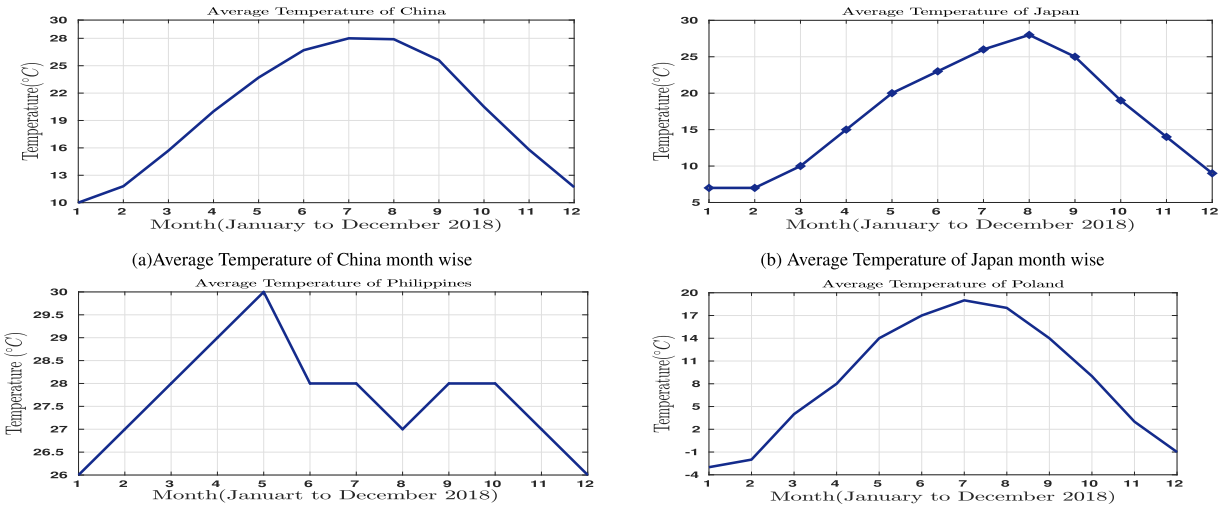

(a)Average Temperature of China month wise

(b) Average Temperature of Japan month wise

(c) Average Temperature of philippines month wise

(d) Average Temperature of Poland month wise

FIGURE 21. Average monthly temperatures recorder in countries with vector-borne diseases. China (a), Japan (b), Philippines (c), Poland (d).

between the WS and the B-A contact network models show that with the homogeneous network model (WS) the peak of the infection is lower than for the heterogeneous one (B-A) and the epidemics propagate slower. These poor estimations of the epidemic dynamics can have a very negative impact on the control policies implementation. In other words, these results highlight the need of more realistic models in order to design and to tune adequately efficient control policies. Our results are based on a generic model. They can be adapted to specific vector-borne disease using an appropriate parameter setting. However, one has to acknowledge that it is not a straightforward issue.

There are various future directions for this work. One of the future direction of this work is to tailor the model to specific vector-borne diseases. This is not a simple issue, because even when data are available, it is not easy to get all the experimental conditions linked to these data. A significant addition is to consider other environmental features such as the impact of humidity. Indeed, most diseases proliferate after the rainy season, where humidity is high, especially in India. More sophisticated models with additional compartmental states can also be easily incorporated. Furthermore, a more realistic scenario can be created by considering the different interplay between hosts such as modular networks and dynamic networks. [68]–[70]. The mobility and spatial distribution of vector, as well as the host population may also be examined by using point of interest based community formation [71], [72].

REFERENCES

[1] E. D'Ortenzio, S. Matheron, X. D. Lamballerie, B. Hubert, G. Piorkowski, M. Maquart, D. Descamps, F. Damond, Y. Yazdanpanah, and I. Leparc-Goffart, "Evidence of sexual transmission of Zika virus," *New England J. Med.*, vol. 374, no. 22, pp. 2195–2198, 2016.

[2] Y. A. Terefe, H. Gaff, M. Kamga, and L. van der Mescht, "Mathematics of a model for Zika transmission dynamics," *Theory Biosci.*, vol. 137, no. 2, pp. 209–218, Nov. 2018.

[3] C. M. Saad-Roy, J. Ma, and P. van den Driessche, "The effect of sexual transmission on Zika virus dynamics," *J. Math. Biol.*, vol. 77, nos. 6–7, pp. 1917–1941, Dec. 2018.

[4] T. Ferdousi, L. W. Cohnstaedt, D. S. McVey, and C. M. Scoglio, "Understanding the survival of Zika virus in a vector interconnected sexual contact network," *Sci. Rep.*, vol. 9, no. 1, pp. 1–15, Dec. 2019.

[5] T. Yildirmak, N. Tulek, and C. Bulut, "Crimean–Congo haemorrhagic fever: Transmission to visitors and healthcare workers," *Infection*, vol. 44, no. 5, pp. 687–689, Oct. 2016.

[6] M. Dutto, M. Bertero, N. Petrosillo, M. Pombi, and D. Otranto, "Ebola virus and arthropods: A literature review and entomological consideration on the vector role," *Bull. De La Société de Pathologie Exotique*, vol. 109, no. 4, pp. 244–247, Oct. 2016.

[7] *Global Strategy for Dengue Prevention and Control 2012-2020*, World Health Org., Geneva, Switzerland, 2012.

[8] W. Martens, T. Jetten, J. Rotmans, and L. Niessen, "Climate change and vector-borne diseases: A global modelling perspective," *Global Environ. change*, vol. 5, no. 3, pp. 195–209, 1995.

[9] D. A. Focks, E. Daniels, D. G. Haile, and J. E. Keesling, "A simulation model of the epidemiology of urban dengue fever: Literature analysis, model development, preliminary validation, and samples of simulation results," *Amer. J. Tropical Med. Hygiene*, vol. 53, no. 5, pp. 489–506, Nov. 1995.

[10] R. Ross, *The Prevention of Malaria*. New York, NY, USA: TheClassics, 2012.

[11] G. Macdonald, *The Epidemiology and Control of Malaria*. Oxford, U.K.: Oxford Univ. Press, 1957.

[12] M. Eder, F. Cortes, N. T. de Siqueira Filha, G. V. A. de França, S. Degroote, C. Braga, V. Ridde, and C. M. T. Martelli, "Scoping review on vector-borne diseases in urban areas: Transmission dynamics, vectorial capacity and co-infection," *Infectious Diseases Poverty*, vol. 7, no. 1, p. 90, Dec. 2018.

[13] T. Britton and A. Traoré, "A stochastic vector-borne epidemic model: Quasi-stationarity and extinction," *Math. Biosci.*, vol. 289, pp. 89–95, Jul. 2017.

[14] M. Arquam, A. Singh, and H. Cherifi, "Integrating environmental temperature conditions into the SIR model for vector-borne diseases," in *Proc. Int. Conf. Complex Netw. Appl.* Cham, Switzerland: Springer, 2019, pp. 412–424.

[15] G. Cimini, T. Squartini, F. Saracco, D. Garlaschelli, A. Gabrielli, and G. Caldarelli, "The statistical physics of real-world networks," *Nature Rev. Phys.*, vol. 1, no. 1, pp. 58–71, Jan. 2019.

[16] M. Jebabli, H. Cherifi, C. Cherifi, and A. Hammouda, "Overlapping community structure in co-authorship networks: A case study," in *Proc. 7th Int. Conf. U- E- Service, Sci. Technol.*, Dec. 2014, pp. 26–29.

[17] M. Jebabli, H. Cherifi, C. Cherifi, and A. Hamouda, "User and group networks on YouTube: A comparative analysis," in *Proc. IEEE/ACS 12th Int. Conf. Comput. Syst. Appl. (AICCSA)*, Nov. 2015, pp. 1–8.

[18] M. Jebabli, H. Cherifi, C. Cherifi, and A. Hamouda, "Community detection algorithm evaluation with ground-truth data," *Phys. A, Stat. Mech. Appl.*, vol. 492, pp. 651–706, Feb. 2018.

[19] A. Singh and Y. N. Singh, "Nonlinear spread of rumor and inoculation strategies in the nodes with degree dependent tie strength in complex networks," *Acta Phys. Polonica B*, vol. 44, no. 1, p. 5, 2013.

[20] R. Albert and A.-L. Barabási, "Statistical mechanics of complex networks," *Rev. Mod. Phys.*, vol. 74, p. 47, Jan. 2002.

[21] G. K. Orman, V. Labatut, and H. Cherifi, "Towards realistic artificial benchmark for community detection algorithms evaluation," 2013, *arXiv:1308.0577*. [Online]. Available: http://arxiv.org/abs/1308.0577

[22] E. A. Mordecai, J. M. Caldwell, M. K. Grossman, C. A. Lippi, L. R. Johnson, M. Neira, J. R. Rohr, S. D. Ryan, V. Savage, M. S. Shocket, R. Sippy, A. M. S. Ibarra, M. B. Thomas, and O. Villena, "Thermal biology of mosquito-borne disease," *Ecol. Lett.*, vol. 22, no. 10, pp. 1690–1708, 2019.

[23] A. T. Ciota, A. C. Keyel, "The role of temperature in transmission of zoonotic arboviruses," *Viruses*, vol. 11, no. 11, p. 1013, Nov. 2019.

[24] C. D. Harvell, C. E. Mitchell, J. R. Ward, S. Altizer, A. P. Dobson, R. S. Ostfeld, and M. D. Samuel, "Climate warming and disease risks for terrestrial and marine biota," *Science*, vol. 296, no. 5576, pp. 2158–2162, 2002.

[25] K. L. Ebi and J. Nealon, "Dengue in a changing climate," *Environ. Res.*, vol. 151, pp. 115–123, Nov. 2016.

[26] X. Wu, Y. Lu, S. Zhou, L. Chen, and B. Xu, "Impact of climate change on human infectious diseases: Empirical evidence and human adaptation," *Environ. Int.*, vol. 86, pp. 14–23, Jan. 2016.

[27] H. Tian, S. Zhou, L. Dong, T. P. Van Boeckel, Y. Cui, S. H. Newman, J. Y. Takekawa, D. J. Prosser, X. Xiao, Y. Wu, B. Cazelles, S. Huang, R. Yang, B. T. Grenfell, and B. Xu, "Avian influenza H5N1 viral and bird migration networks in Asia," *Proc. Nat. Acad. Sci. USA*, vol. 112, no. 1, pp. 172–177, Jan. 2015.

[28] C. J. Portier, K. T. Tart, S. R. Carter, C. H. Dilworth, A. E. Grambsch, J. Gohlke, J. Hess, S. N. Howard, G. Luber, and J. T. Lutz, "A human health perspective on climate change: A report outlining the research needs on the human health effects of climate change," *J. Current Issues Globalization*, vol. 6, no. 4, p. 621, 2013.

[29] K. L. Gage, T. R. Burkot, R. J. Eisen, and E. B. Hayes, "Climate and vectorborne diseases," *Amer. J. Preventive Med.*, vol. 35, no. 5, pp. 436–450, Nov. 2008.

[30] *Using Climate To Predict Infectious Disease Epidemics*, World Health Org., Geneva, Switzerland, 2005.

[31] H. Xiao, H.-Y. Tian, L.-D. Gao, H.-N. Liu, L.-S. Duan, N. Basta, B. Cazelles, X.-J. Li, X.-L. Lin, H.-W. Wu, B.-Y. Chen, H.-S. Yang, B. Xu, and B. Grenfell, "Animal reservoir, natural and socioeconomic variations and the transmission of hemorrhagic fever with renal syndrome in Chenzhou, China, 2006–2010," *PLoS Neglected Tropical Diseases*, vol. 8, no. 1, p. e2615, Jan. 2014.

[32] S. Dickin, "Assessing vulnerability to water-associated disease: An ecosystem approach to health," Ph.D. dissertation, MacSphere, McMaster Univ., Hamilton, ON, Canada, 2014.

[33] A. Egizi, N. H. Fefferman, and D. M. Fonseca, "Evidence that implicit assumptions of 'no evolution' of disease vectors in changing environments can be violated on a rapid timescale," *Philos. Trans. Roy. Soc. B, Biol. Sci.*, vol. 370, no. 1665, Apr. 2015, Art. no. 20140136.

[34] P. E. Parham, J. Waldock, G. K. Christophides, and E. Michael, "Climate change and vector-borne diseases of humans," Roy. Soc. Publ., London, U.K., Tech. Rep. 10.1098/rstb.2014.0377, 2015.

[35] L. P. Campbell, C. Luther, D. Moo-Llanes, J. M. Ramsey, R. Danis-Lozano, and A. T. Peterson, "Climate change influences on global distributions of dengue and Chikungunya virus vectors," *Philos. Trans. Roy. Soc. B, Biol. Sci.*, vol. 370, no. 1665, Apr. 2015, Art. no. 20140135.

[36] S. A. Moon, L. W. Cohnstaedt, D. S. McVey, and C. M. Scoglio, "A spatio-temporal individual-based network framework for west Nile virus in the USA: Spreading pattern of west Nile virus," *PLOS Comput. Biol.*, vol. 15, no. 3, Mar. 2019, Art. no. e1006875.

[37] M. Sekamatte, M. H. Riad, T. Tekleghiorghis, K. J. Linthicum, S. C. Britch, J. A. Richt, J. P. Gonzalez, and C. M. Scoglio, "Individual-based network model for rift valley fever in Kabale district, Uganda," *PLoS ONE*, vol. 14, no. 3, Mar. 2019, Art. no. e0202721.

[38] W. Wang and G. Mulone, "Threshold of disease transmission in a patch environment," *J. Math. Anal. Appl.*, vol. 285, no. 1, pp. 321–335, 2003.

[39] J. Arino and P. van den Driessche, "A multi-city epidemic model," *Math. Population Stud.*, vol. 10, no. 3, pp. 175–193, Jan. 2003.

[40] J. Arino, R. Jordan, and P. van den Driessche, "Quarantine in a multi-species epidemic model with spatial dynamics," *Math. Biosci.*, vol. 206, no. 1, pp. 46–60, Mar. 2007.

[41] P. Auger, E. Kouokam, G. Sallet, M. Tchuente, and B. Tsanou, "The Ross–Macdonald model in a patchy environment," *Math. Biosci.*, vol. 216, no. 2, pp. 123–131, Dec. 2008.

[42] D. Soriano-Paños, J. H. Arias-Castro, A. Reyna-Lara, H. J. Martínez, S. Meloni, and J. Gómez-Gardeñes, "Vector-borne epidemics driven by human mobility," *Phys. Rev. Res.*, vol. 2, no. 1, Mar. 2020, Art. no. 013312.

[43] G. R. Phaijoo and D. B. Gurung, "Mathematical study of dengue disease transmission in multi-patch environment," *Appl. Math.*, vol. 7, no. 14, pp. 1521–1533, 2016.

[44] M. Nekovee, Y. Moreno, G. Bianconi, and M. Marsili, "Theory of rumour spreading in complex social networks," *Phys. A, Stat. Mech. Appl.*, vol. 374, no. 1, pp. 457–470, Jan. 2007.

[45] A. Singh and Y. N. Singh, "Rumor spreading and inoculation of nodes in complex networks," in *Proc. 21st Int. Conf. Companion World Wide Web (WWW Companion)*, 2012, pp. 675–678.

[46] R. Pastor-Satorras, C. Castellano, P. Van Mieghem, and A. Vespignani, "Epidemic processes in complex networks," *Rev. Mod. Phys.*, vol. 87, no. 3, p. 925, 2015.
[47] Z. Wang, C. T. Bauch, S. Bhattacharyya, A. D'Onofrio, P. Manfredi, M. Perc, N. Perra, M. Salathé, and D. Zhao, "Statistical physics of vaccination," *Phys. Rep.*, vol. 664, pp. 1–113, Dec. 2016.
[48] A. Vespignani, "Modelling dynamical processes in complex socio-technical systems," *Nature Phys.*, vol. 8, no. 1, pp. 32–39, Jan. 2012.
[49] A. Saumell-Mendiola, M. Á. Serrano, and M. Boguñá, "Epidemic spreading on interconnected networks," *Phys. Rev. E, Stat. Phys. Plasmas Fluids Relat. Interdiscip. Top.*, vol. 86, no. 2, Aug. 2012, Art. no. 026106.
[50] S. Hong, H. Yang, T. Zhao, and X. Ma, "Epidemic spreading model of complex dynamical network with the heterogeneity of nodes," *Int. J. Syst. Sci.*, vol. 47, no. 11, pp. 2745–2752, Aug. 2016.
[51] C. Castellano and R. Pastor-Satorras, "Thresholds for epidemic spreading in networks," *Phys. Rev. Lett.*, vol. 105, no. 21, Nov. 2010, Art. no. 218701.
[52] M. Li and X. Liu, "An SIR epidemic model with time delay and general nonlinear incidence rate," *Abstract Appl. Anal.*, vol. 2014, pp. 1–7, Feb. 2014.
[53] M. Arquam, A. Singh, and R. Sharma, "Modelling and analysis of delayed sir model on complex network," in *Proc. Int. Conf. Complex Netw. Appl.* Cham, Switzerland: Springer, 2018, pp. 418–430.
[54] S. Huang and J. Jiang, "Epidemic dynamics on complex networks with general infection rate and immune strategies," *Discrete Continuous Dyn. Syst.-B*, vol. 23, no. 6, p. 2071, 2018.
[55] S. Hosseini and M. A. Azgomi, "The dynamics of an SEIRS-QV malware propagation model in heterogeneous networks," *Phys. A, Stat. Mech. Appl.*, vol. 512, pp. 803–817, Dec. 2018.
[56] R. Zhou and Q. Wu, "Epidemic spreading dynamics on complex networks with adaptive social-support," *Phys. A, Stat. Mech. Appl.*, vol. 525, pp. 778–787, Jul. 2019.
[57] A. I. Dell, S. Pawar, and V. M. Savage, "Systematic variation in the temperature dependence of physiological and ecological traits," *Proc. Nat. Acad. Sci. USA*, vol. 108, no. 26, pp. 10591–10596, Jun. 2011.
[58] P. Amarasekare and V. Savage, "A framework for elucidating the temperature dependence of fitness," *Amer. Naturalist*, vol. 179, no. 2, pp. 178–191, Feb. 2012.
[59] R. B. Huey and J. G. Kingsolver, "Variation in universal temperature dependence of biological rates," *Proc. Nat. Acad. Sci. USA*, vol. 108, no. 26, pp. 10377–10378, Jun. 2011.
[60] E. A. Mordecai, J. M. Cohen, M. V. Evans, P. Gudapati, L. R. Johnson, C. A. Lippi, K. Miazgowicz, C. C. Murdock, J. R. Rohr, S. J. Ryan, V. Savage, M. S. Shocket, A. S. Ibarra, M. B. Thomas, and D. P. Weikel, "Detecting the impact of temperature on transmission of Zika, dengue, and Chikungunya using mechanistic models," *PLOS Neglected Tropical Diseases*, vol. 11, no. 4, Apr. 2017, Art. no. e0005568.
[61] G. Magombedze, N. M. Ferguson, and A. C. Ghani, "A trade-off between dry season survival longevity and wet season high net reproduction can explain the persistence of anopheles mosquitoes," *Parasites Vectors*, vol. 11, no. 1, p. 576, Dec. 2018.
[62] X. Liu, T. Li, X. Cheng, W. Liu, and H. Xu, "Spreading dynamics of a preferential information model with hesitation psychology on scale-free networks," *Adv. Difference Equ.*, vol. 2019, no. 1, p. 279, Dec. 2019.
[63] A. Ibnoulouafi, M. El Haziti, and H. Cherifi, "M-centrality: Identifying key nodes based on global position and local degree variation," *J. Stat. Mech., Theory Exp.*, vol. 2018, no. 7, Jul. 2018, Art. no. 073407.
[64] J. P. Messina, M. U. Kraemer, O. J. Brady, D. M. Pigott, F. M. Shearer, D. J. Weiss, N. Golding, C. W. Ruktanonchai, P. W. Gething, E. Cohn, J. S. Brownstein, K. Khan, A. J. Tatem, T. Jaenisch, C. J. Murray, F. Marinho, T. W. Scott, and S. I. Hay, "Mapping global environmental suitability for Zika virus," *ELife*, vol. 5, Apr. 2016, Art. no. e15272.
[65] L. Eisen, A. J. Monaghan, S. Lozano-Fuentes, D. F. Steinhoff, M. H. Hayden, and P. E. Bieringer, "The impact of temperature on the bionomics of Aedes (Stegomyia) aegypti, with special reference to the cool geographic range margins," *J. Med. Entomol.*, vol. 51, no. 3, pp. 496–516, May 2014.
[66] J. Liu-Helmersson, H. Stenlund, A. Wilder-Smith, and J. Rocklöv, "Vectorial capacity of Aedes aegypti: Effects of temperature and implications for global dengue epidemic potential," *PLoS ONE*, vol. 9, no. 3, Mar. 2014, Art. no. e89783.
[67] S. Polwiang, "The seasonal reproduction number of dengue fever: Impacts of climate on transmission," *PeerJ*, vol. 3, p. e1069, Jul. 2015.
[68] K. Orman, V. Labatut, and H. Cherifi, "An empirical study of the relation between community structure and transitivity," in *Complex Networks* (Studies in Computational Intelligence), vol. 424, R. Menezes, A. Evsukoff, and M. González, Eds. Berlin, Germany: Springer, 2013, pp. 99–110.
[69] N. Gupta, A. Singh, and H. Cherifi, "Centrality measures for networks with community structure," *Phys. A, Stat. Mech. Appl.*, vol. 452, pp. 46–59, Jun. 2016.
[70] Z. Ghalmane, M. El Hassouni, C. Cherifi, and H. Cherifi, "Centrality in modular networks," *EPJ Data Sci.*, vol. 8, no. 1, p. 15, Dec. 2019.
[71] X. Xiong, S. Qiao, Y. Li, N. Han, G. Yuan, and Y. Zhang, "A point-of-interest suggestion algorithm in multi-source geo-social networks," *Eng. Appl. Artif. Intell.*, vol. 88, 2020, Art. no. 103374.
[72] X. Xiong, S. Qiao, N. Han, F. Xiong, Z. Bu, R.-H. Li, K. Yue, and G. Yuan, "Where to go: An effective point-of-interest recommendation framework for heterogeneous social networks," *Neuro Comput.*, vol. 373, pp. 56–69, 2020.

MD ARQUAM is currently pursuing the Ph.D. degree with the Department of Computer Science and Engineering, National Institute of Technology Delhi, India. He has authored or coauthored more than seven technical articles in major international conferences. His research interests include dynamics on and of networks, random geometry, epidemic spreading on networks, and wireless sensor networks. He has attended various workshops and summer schools over diversified subjects.

ANURAG SINGH (Senior Member, IEEE) is currently an Assistant Professor at the Department of Computer Science and Engineering, National Institute of Technology Delhi, India. He has authored or coauthored over 42 technical articles in major international journals and conferences. His research interests include complex networks, dynamics of information in complex networks, graph spectra, attacks on complex networks, time varying networks, community structure, and game theory. He currently serves as a reviewer of many international journals and conferences.

HOCINE CHERIFI received the Ph.D. degree from the National Polytechnic Institute, Grenoble, in 1984. He has been a Full Professor of computer science at the University of Burgundy, Dijon, France, since 1999. Prior to moving to Dijon, he held faculty positions at Rouen University and Jean Monnet University, France. He has held visiting positions at Yonsei, Korea, The University of Western Australia, Australia, National Pingtung University, Taiwan, and Galatasaray University, Turkey. He has published more than 200 scientific articles in international refereed journals and conference proceedings. His recent research interests include computer vision and complex networks. He held leading positions in more than 15 international conference organization, as the General Chair and the Program Chair, and he served in MORE than 100 program committee. He is the Founder of the International Conference on Complex Networks & their Applications. He is currently a member of the Editorial Board of *Computational Social Networks*, *PLOS One*, IEEE Access, *Journal of Imaging*, *Complex Systems*, *Quality & Quantity*, and *Scientific Reports*. He is the Founding Editor-in-Chief of *Applied Network Science* journal.